CSCE 2022 Annual Conference
Whistler, British Columbia
May 25th – 28th, 2022

Finite Element Modeling of Fiber Reinforced Polymer Composite Tubes Filled with Concrete

Sadat Hosseini, Alireza[1,2] and Sadeghian, Pedram[1]
[1] Department of Civil and Resource Engineering, Dalhousie University, Canada
[2] corresponding_author_ asadat@dal.ca

Abstract: Sustainable development of Civil Engineering infrastructure has already benefited from the use of fiber-reinforced polymer (FRP) composite materials for different structural applications such as reinforcing existing structures and constructing new ones. Among the various FRP structural elements, ±55˚ filament wound glass FRP (GFRP) tubes, which are typically prefabricated for piping application, have been considered in a number of structural applications. As a load-bearing structural element, filling these tubes with concrete (concrete-filled FRP tubes or CFFTs) can considerably enhance their stiffness and strength under axial and flexural loadings. Although there have been multiple studies on the bending and compressive behavior of CFFTs, studies on the tensile behavior of CFFTs and especially those made of ±55˚ GFRP tubes are quite scarce. Here in this study, in order to take a step toward a better understanding of the behavior of the CFFTs under axial tension, finite element models of the hollow tubes and CFFTs were generated using the ABAQUS software package and verified against the experimental outputs of previous studies. Shell elements were used to model the tube while solid elements formed the concrete. The concrete damaged plasticity (CDP) model was used to introduce the material properties of the concrete to the model. Quasi-static analysis using Dynamic/Explicit solver was implemented due to its capabilities for converging highly non-linear problems. Good compatibility of the results of the numerical study with the test outputs was seen on both hollow tubes and CFFTs. It can be concluded that the damage criteria used for FRP were capable of predicting matrix cracking as the governing mode of failure in FRP observed in the experiments. Moreover, the CDP model could simulate the tensile cracking of concrete.

Keywords: GFRP Tube, Concrete, CFFT, Tension, Finite Element Analysis

1 INTRODUCTION

Filament wound fiber-reinforced polymer (FRP) tubes have recently been used instead of traditional metallic pipes in municipal sectors. This has improved the importance of these pipes and therefore, they have been extensively studied under internal and external pressure loading by some researchers (Xing et al. 2015; Rafiee 2016). However, there are quite scarce studies on the axial behavior of filament-wound glass fiber-reinforced polymer (GFRP) tubes and further studies and investigations, which is the purposes of this study, are required to shed more light on the mechanical behavior of these tubes in order to be used in a wide variety of structures. In an experimental study by Bai et al. (1997), the mechanical behavior of filament-wound GFRP tubes was investigated under pure axial tensile load, pure internal pressure, and combined loading. Results of this study were used to recognize the main damage initiation mechanisms such as micro-cracking and delamination. The researchers of another study, Khalifa et al. (2012) experimentally investigated the mechanical behavior of filament wound tubes under axial monotonic loading. Through this study, a non-destructive test was developed whose results were in line with the traditional tensile tests. One of the very recent studies on the axial (Betts et al. 2019) and flexural (Betts et al. 2021) behavior of these tubes was conducted in the Department of Civil and Resource Engineering, Dalhousie University. Experimental and analytical investigation of the behavior of these tubes under longitudinal compressive and tensile loading. According to the experiments, it was seen that the failure started with matrix cracking along the direction of the fibers and continued until the specimen fails. Through the analytical studies, nonlinear formulations were presented on the behavior of the tubes and verified against the experiments and the literature. A clear understanding of the material behavior and the response of these tubes under different loading conditions is provided which is the basis of further investigation on these tubes.

Although very good studies have been done so far on the behavior of filament-wound GFRP tubes, albeit limited, investigation of the behavior of concrete-filled tubes (CFFTs) is much more limited. The idea of CFFTs was proposed by Mirmiran and Shahawy (1996) inspired by the concrete-filled steel tubes to achieve high strength, ductility and prolonged durability. Fam and Rizkalla (2002) conducted large-scale tests on concrete-filled GFRP tubes. They targeted the strength to weight ratio and found that specimens with a central longitudinal hole are the optimum scheme. The contribution of concrete to the flexural strength was studied and a parametric study on the effective parameters was carried on. In another research by Fam et al. (2003), the behavior of CFFTs was studied through an experimental program, and an analytical model was proposed. It was found that increasing the ratio of fibers in the axial direction enhances the flexural strength, while axial compressive strength of CFFTs increased when higher ratios of fibers in the hoop direction were used. Shao and Mirmiran (2005) studied the cyclic behavior of CFFTs as simple span beam-columns. Half of the specimens were filament wounds and others were centrifuge casting tubes. Thick tubes failed with a brittle compression mode while a ductile tension failure was observed in thin tubes. In another study by Zohrevand and Mirmiran (2013), Ultra high-performance concrete-filled fiber-reinforced polymer tubes (UHPCFFT) were studied to estimate their maximum ground acceleration capacity as column members. Although the ductility of the un-reinforced CFFTs was lower than the reinforced ones, higher ground acceleration capacity was observed for the thinnest CFFT with no steel reinforcement.

More recently, Qasrawi et al. (2015) studied the behavior of CFFTs under dynamic impact loads and presented a procedure for the analysis and design of CFFTs under this type of loading. Promising results were achieved regarding the flexural capacity and maximum displacement for CFFTs over the conventional reinforced concrete counterparts. Using existing experimental data Li et al. (2016) on seawater and sea sand concrete (SWSSC) with FRP tubes, Li et al. (2018) presented a theoretical model to present the behavior of these CFFTs. The model was developed on an existing dilation model for concrete-filled FRP wraps (Teng et al. 2007) combined with a biaxial stress analysis to incorporate the effect of the Poisson's ratio of the tubes in the model. Xie et al. (2020) investigated the behavior of the CFFTs under axial compressive loading through experiments and developed an analytical model to capture the nonlinear biaxial behavior of concrete-filled filament-wound FRP confining tubes. Lu and Fam (2020) experimentally investigated the effect of damage on the FRP tubes of CFFTs in form of controlled longitudinal and circumferential linear cuts on the flexural strength of these tubes. Cross-ply tubes were found to be more vulnerable in comparison to the angle-ply commercially used tubes. Moreover, tension side cuts were more effective in strength reduction than compression side cuts. Jawdhari et al. (2020) conducted numerical studies CFFTs under axial load and bending moment. ANSYS and LS DYNA software packages were used

for the simulations. Although LS DYNA results followed the overall trend of the test results, the model had some deviations regarding the stresses corresponding to concrete splitting crack and stiffness reduction.

An overall review of the past studies reveals that not only our knowledge about the structural behavior of the CFFTs is not enough, but also studies on ±55˚ filament wound GFRP tubes under tensile loading have not yet moved much towards a deeper understanding of their behavior when filled with concrete. This study aims to develop a finite element model using the ABAQUS software package (ABAQUS/Standard User's Manual 2014) to simulate the behavior of CFFTs under axial tension. The geometrical and mechanical properties of the GFRP and concrete were introduced to the model based on the available experimental data. First, the finite element model of the hollow tube was generated and verified against the experiments. Then the concrete part was added to the model and analyzed. Results of the finite element models were in good agreement with the experiments regarding the prediction of tube stiffness and failure patterns.

2 BENCHMARK EXPERIMENTS

The experimental outputs were taken from two separate studies, one on the hollow GFRP tubes under tensile loading, and the other one on the CFFTs under tension. An innovative test method of capturing the tensile behavior was proposed (Betts et al. 2019) to investigate the behavior of hollow tubes under axial tensile loading. In this method, the actual tensile parameters are driven from the full pipe test instead of coupons with some shortcomings such as fiber discontinuity along the edges. Tubes with different diameter to thickness ratios (DTR) and nominal pressure ratings (NPR) were selected for the experiments. Among these tubes, P1050-D76-T with the geometrical properties presented in Table 1 was selected to be filled with concrete in another study (Khan 2019). The concrete mix design was designed to reach a compressive strength of about 40 MPa. Concrete cylinder specimens were made of the manufactured concrete mix and tested according to ASTM C39 (American Society for Testing and Materials 2014) to determine the compressive strength of concrete. The value of the compressive strain was found to be around 38 MPa which was acceptable. The same concrete was poured inside the tube and cured at room temperature for 28 days while covered with plastic sheets and then tested. Before filling the tubes with concrete, the inside surface of the tube's wall was greased to achieve a smooth and frictionless surface. Two steel cores with steel rods were used on the top and bottom of the tube to make it possible for tensile testing.

Table 1: Structural and geometrical properties of P1050-D76-T

Nominal Pressure Rating (kPa)	Inner Diameter (mm)	Cross Sectional Area (mm2)	Wall Thickness (mm)	Filament Wind Layup (°)
1050	76.2	964.4	3.8	[±55]7

The test specimens were fixed inside a 2MN Static Hydraulic Universal Testing System, and the steel rods of the specimen were attached to the plates of the testing machine. The specimens were subjected to tensile loading at a rate of 2 mm/min, and the load-displacement and the strains of the specimen were measured using a data acquisition system collecting data every 1/10 seconds. The test setup can be found in Betts et al. (2019). The tension tests were continued after peak load up to the point that the load decreased to 80% of the peak load. According to the experiments, the failure in hollow GFRP tubes is in the form of matrix cracking which follows the directions of the fibers at ±55°. The failure in GFRP for the CFFT sample was mostly at the ends adjacent to the steel cores mainly because of using concrete that controls the biaxial strains. For the concrete core, cracking in the middle due to the tensile failure and crushing in both ends due to the compressive failure were observed.

3 FINITE ELEMENT SIMULATION

3.1 Material Parameters

The material properties of the GFRP based on the manufacturer data were taken from one of the reference studies (Betts et al. 2019) for this research and are presented in Table 2.

Table 2: The verified material properties of GFRP

Property	Value	Property	Value
E1	40000	SL+	1036
E2	9500	SL-	567
υ12	0.28	ST+	50
G12	3900	ST-	116
G23	2700	SLT	81

E1: Longitudinal Elastic Modulus; E2: Transverse Elastic Modulus; G12: Shear Modulus; v12: Major Poisson's Ratio; v21: Minor Poisson's Ratio; SL+: Longitudinal Tensile Strength; SL-: Longitudinal Compressive Strength; ST+: Transverse Tensile Strength; ST-: Transverse Compressive Strength; SLT: Shear Strength.

Hashin damage criteria (Hashin 1980) were used in the numerical models to consider the strength of the GFRP tube taking into account the material properties given in Table 2. The post-damage behavior of the FRP elements was considered in the analyses to cater for damage evolution.

The concrete material was modeled using the concrete damaged plasticity (CDP) model in ABAQUS having a compressive strength (f'_c) of 38 MPa based on the experimental data. The CDP model is a continuum, plasticity-based, damage model for concrete. It assumes that the main two failure mechanisms are tensile cracking and compressive crushing of the concrete material. The model assumes that the uniaxial tensile and compressive response of concrete is characterized by damaged plasticity. To introduce the concrete damage properties to ABAQUS, it is needed to introduce the modulus of elasticity (E_c) and the Poisson's ratio (v). According to ACI 318–08 (American Concrete Institute 2008), for normal-weight concrete, the modulus of elasticity of concrete is:

[1] $E_c = 4700 \sqrt{f'_c} = 4700 \times \sqrt{38} \approx 29000$ MPa

For the design of concrete structures, the most common value of concrete Poisson's ratio is taken as 0.2. To define the compressive behavior and the corresponding compressive crushing or the tensile behavior and its corresponding tensile cracking, two curves are needed to be defined for each compressive and tensile behavior: Yield Stress vs. Inelastic Strain and Damage Parameter vs. Inelastic Strain. Inelastic Strain is calculated by the following formulation:

[2] $\varepsilon^{in} = \varepsilon - \sigma/E_c$

Wherein, ε and σ are the concrete strain and stress, respectively. The inelastic strain in the tensile behavior is known as the cracking strain. When extracting the inelastic strain from the initial stress-strain data, the yield stress could be found from the stress-strain curve which is the stress value corresponding to the shift from the linear response to nonlinear. The Damage Parameter (d) is calculated using the ratio of concrete stress (σ) and concrete yield stress (σ_y):

[3] $d = 1 - \sigma/\sigma_y$

In order to introduce the tensile behavior of concrete, its tensile strength can be calculated using the following relationship between the splitting tensile strength and compressive strength according to ACI 318 (American Concrete Institute 2008):

[4] $f_t = 0.56 \sqrt{f'_c} = 0.56 \times \sqrt{38} \approx 3.5$ MPa

Table 3 presents the material properties of the concrete for the CDP model.

Table 3: Material properties of the concrete core in the finite element model

Property	Value	Property	Value
Dilation angle	35˚	Mass density (Kg/m^3)	2300
Eccentricity	0.1	Young's modulus (MPa)	28970
$F=\sigma_{bo}/\sigma_{co}$	1.16	Poisson's ratio	0.2
K_c	0.667	Compressive and Tensile strength (MPa)	38 and 3.5

3.2 Geometry and Boundary Conditions

The geometries of the finite element models are similar to the experimental samples, P1050-D76-T, presented in Table 1. The Inner Diameter of the tube is 76.2 mm, the wall thickness is 3.8 mm, and its length was assumed 450 mm. Two circular rigid plates were used in the models representing the experimental steel caps of the specimens. Shell elements type S8 in ABAQUS were used to generate the tube, while Solid elements type C3D8 in ABAQUS were used for the concrete fill geometry in the finite element models. The finite element models of the hollow tube and CFFT are presented in Figure 1.

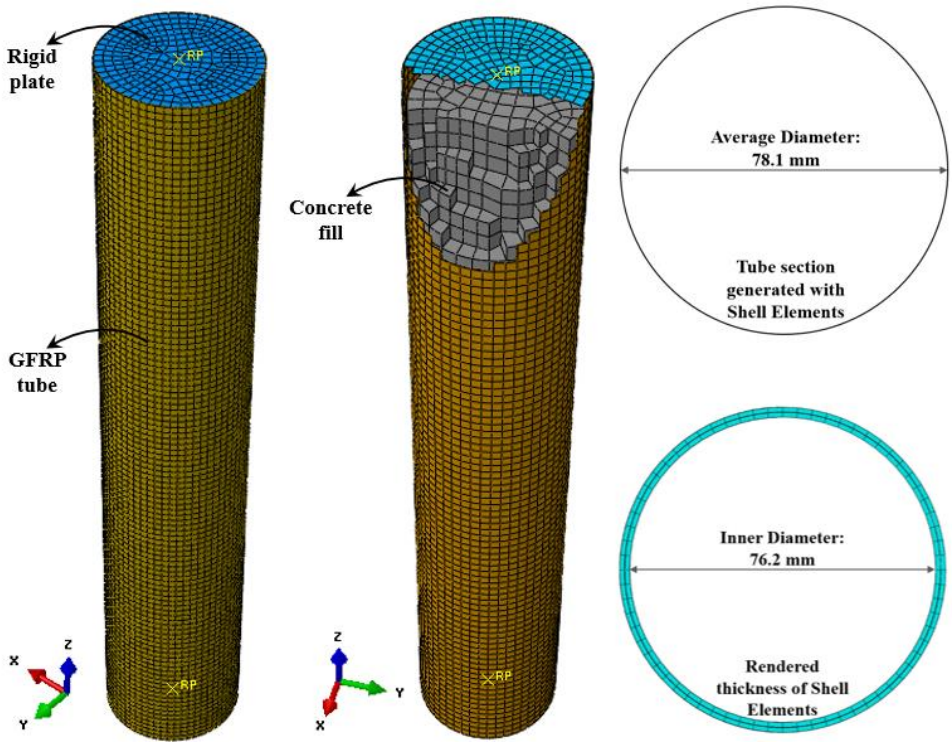

Figure 1: Schematic diagram of the reshaping of (a) Hollow GFRP tube and (b) CFFT

The layup configuration of the filament wound GFRP tube was introduced to the model based on the data obtained from the manufacturer of the filament wound ±55˚ GFRP tubes as per Table 1. Figure 2 presents the GFRP layup of the P1050-D76-T tube in the finite element model.

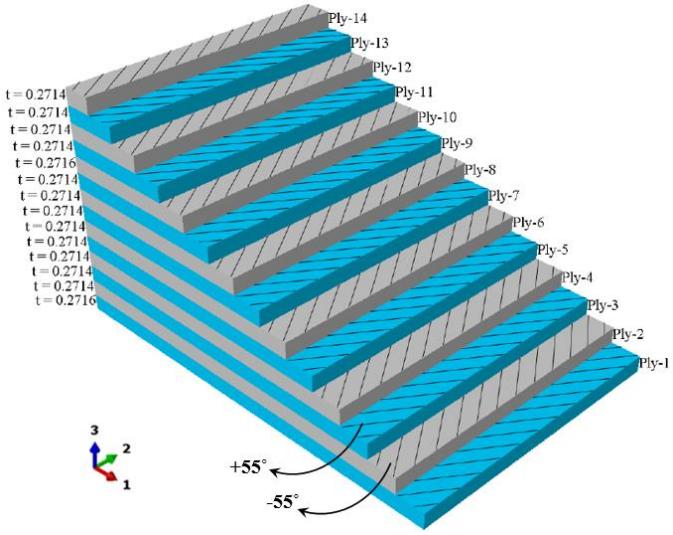

Figure 2: The composite layup in the numerical model

The boundary conditions of the model were chosen as close as possible to the experimental setup. The plate on the top end acted as the load cell (applying the tensile load). An increasing time-dependent displacement was applied on the top rigid plate, while the bottom one restricted all degrees of freedom of the tube. Since oil was used to cover the inside surface of the tube in the experiments, surface-to-surface contact with frictionless contact material was used to simulate the friction of concrete with the inner surface of the tube in the finite element models. The modeling was conducted using Quasi-static analysis using Dynamic/Explicit solver of ABAQUS which includes the loading speed and the materials' density and is capable of solving non-linear and complicated problems.

4 RESULTS AND DISCUSSION

This section is divided into two subsections, presenting the results of finite element modeling of the hollow tubes and CFFTs.

4.1 Hollow Tube

Figure 3a illustrates the stress-strain curve of the filament wound GFRP tubes resulting from the finite element modeling of the hollow tubes. As can be seen, the model could simulate the tube stiffness, strength and post-failure behavior with good accuracy in comparison to the test result. Figure 3b shows the damage contours of the hollow tubes and the concrete-filled ones under the axial tension. As can be seen in this figure, the numerical finite element model could capture the damage mechanism as similar to the observations of the experiments. The failure in the tube is in the form of matrix cracking along the direction of the fibers which continues until the failure of the tube.

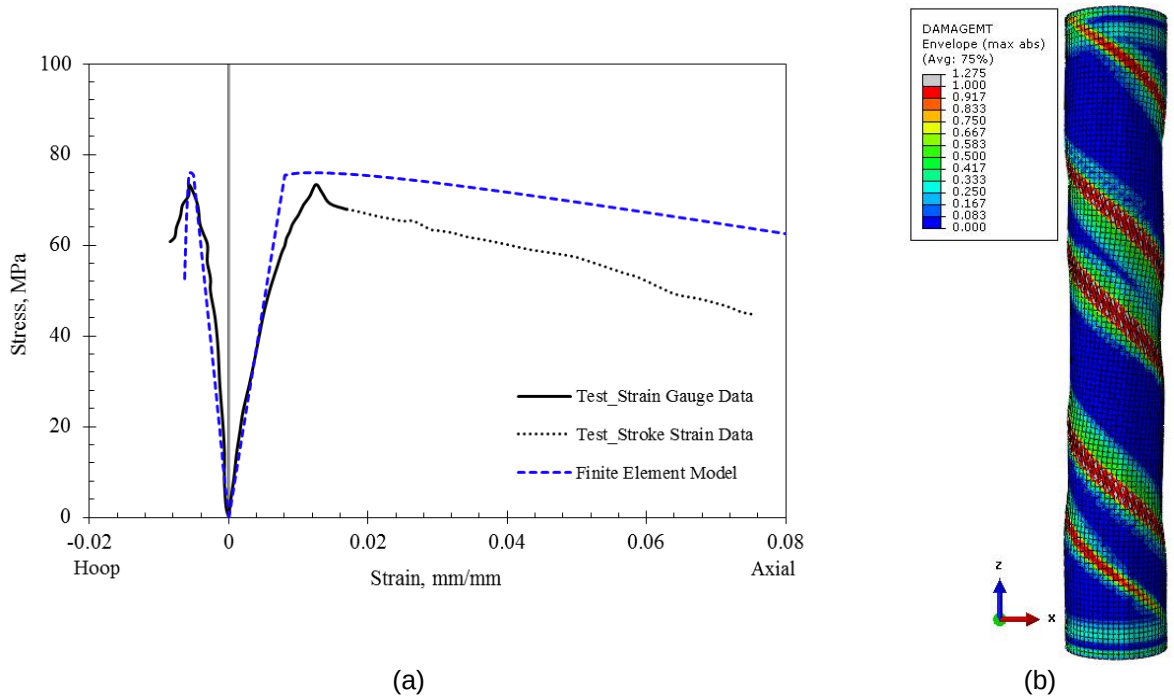

(a) (b)

Figure 3: Results of the finite element modeling of the hollow GFRP tube: a) Comparing the test results (Betts et al. 2019) with the ABAQUS numerical model, b) Damage contours of GFRP matrix in tension

4.2 Concrete-Filled FRP Tube (CFFT)

Figure 4a illustrates the stress-strain relationship of the finite element model and the experiments on the concrete-filled FRP tubes (CFFT), and Figure 4b shows the damage contours of the concrete core at the end of the tensile loading. The difference between the two tests is that in Test#2 CFRP wraps were used at the ends of the specimen to prevent premature failure at the end. The numbers inside the circles in these figures correspond to the sequence of damage in the concrete core. Point #1 in Figure 4b shows the tensile cracking of concrete in the middle which corresponds to the drop of the stress-strain curve of Figure 4a around 40 to 60 MPa. As it is seen, the finite element model could capture the load-bearing drop of the CFFT which was observed in the experiments. By increasing the tensile load after the drop point, to about 80 kN (Point #2 in Figure 4a), the first damage and stiffness degradations in the GFRP tube occurred, and some other parts of the concrete were damaged (Point #2 in Figure 4b). Therefore, the effectiveness of the concrete in restricting the transverse displacement and necking of the tube decreased. Therefore, the stiffness of the CFFT model dropped to around 80 to 100 kN. The other interesting result which can be seen in Figure 4a is that the FE model could be able to capture the post-failure behavior of the CFFT up to the failure point (Point#3) with acceptable precision in comparison with the outputs of the tests. Overall, comparing the stress-strain diagram of the model and the experiments, it can be seen that there is good compatibility between the model and the experiment.

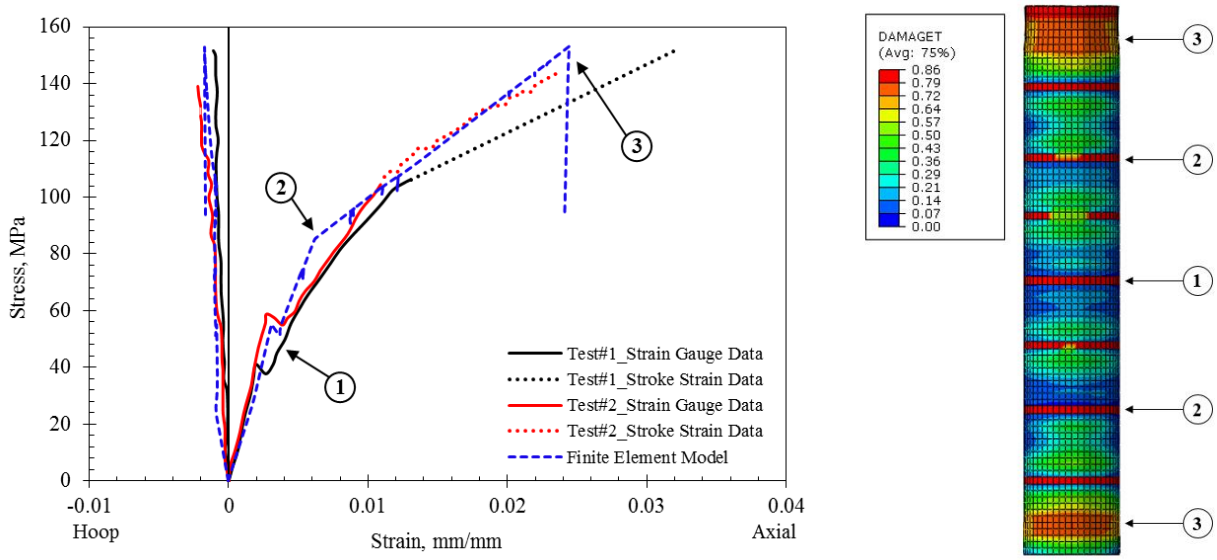

(a) (b)

Figure 4: Results of the finite element modeling of CFFT: a) Comparing the test results (Khan 2019) with the ABAQUS numerical model, b) Damage contours of the concrete core

5 SUMMARY AND CONCLUSION

This paper presents the results of finite element modeling of the concrete-filled GFRP tubes (CFFT). The study started with numerical modeling of the hollow tubes based on the experiments on these tubes. Results showed that the FE model is capable of simulating the behavior of the tubes under tensile loading. Hashin damage criteria for fiber and matrix failure were introduced to the model which could predict the damage pattern of the tube compatible with the experimental observations. Moreover, the CFFT model was generated using the Concrete Damaged Plasticity model in ABAQUS for the concrete core. Results were in good agreement with the experimental outputs regarding the initial damage and its propagation in the concrete core, failures in the FRP in the form of matrix cracking, and post-failure behavior of the CFFT observed in the stress-strain relationship diagram.

This study can be extended to evaluate the effect of the contributing parameters of GFRP and concrete in the finite element model as future research work.

Acknowledgements

The authors of this paper highly appreciate the efforts that were taken by Dillon Betts and Sania Khan in conducting the experiments on hollow and concrete-filled tubes at Dalhousie University.

References

ABAQUS/Standard User's Manual (2014) Version 6.14. Providence, RI: Simulia

American Concrete Institute (2008) Building code requirements for structural concrete (ACI 318-08) and commentary. American Concrete Institute

American Society for Testing and Materials (2014) ASTM C39 / C39M, Standard Test Method for Compressive Strength of Cylindrical Concrete Specimens

Bai J, Seeleuthner P, Bompard P (1997) Mechanical behaviour of ± 55 ° filament-wound glass-

fibre/epoxy-resin tubes: I. Microstructural analyses, mechanical behaviour and damage mechanisms of composite tubes under pure tensile loading, pure internal pressure, and combined loading. Compos Sci Technol 57:141–153. https://doi.org/https://doi.org/10.1016/S0266-3538(96)00124-8
Betts D, Sadeghian P, Fam A (2019) Investigation of the stress-strain constitutive behavior of±55° filament wound GFRP pipes in compression and tension. Compos Part B Eng 172:243–252
Betts D, Sadeghian P, Fam A (2021) Experimental and analytical investigations of the flexural behavior of hollow±55° filament wound GFRP tubes. Thin-Walled Struct 159:107246
Fam A, Flisak B, Rizkalla S (2003) Experimental and analytical modeling of concrete-filled FRP tubes subjected to combined bending and axial loads. ACI Struct J 100:499–509
Fam AZ, Rizkalla SH (2002) Flexural behavior of concrete-filled fiber-reinforced polymer circular tubes. J Compos Constr 6:123–132
Hashin Z (1980) Failure criteria for unidirectional fiber composites. ASME J Appl Mech
Jawdhari A, Fam A, Sadeghian P (2020) Modeling the Nonlinear Response of ±55 Angle-Ply GFRP Tube used in CFFT Applications. In: 8th International Conference on Advanced Composite Materials in Bridges and Structures. Sherbrooke, Quebec, Canada
Khalifa A Ben, Zidi M, Abdelwahed L (2012) Mechanical characterization of glass/vinylester ±55° filament wound pipes by acoustic emission under axial monotonic loading. Comptes Rendus Mécanique 340:453–460. https://doi.org/https://doi.org/10.1016/j.crme.2012.02.006
Khan S (2019) Structural Properties of Commercially Used ±55˚ Filament Wound GFRP Pipes Filled with Concrete in Tension. In partial fulfillment of the requirements of the Engineering Co-op Education Program at Dalhousie University.
Li YL, Teng JG, Zhao XL, Singh Raman RK (2018) Theoretical model for seawater and sea sand concrete-filled circular FRP tubular stub columns under axial compression. Eng Struct 160:71–84. https://doi.org/https://doi.org/10.1016/j.engstruct.2018.01.017
Li YL, Zhao XL, Singh RKR, Al-Saadi S (2016) Experimental study on seawater and sea sand concrete filled GFRP and stainless steel tubular stub columns. Thin-Walled Struct 106:390–406
Lu C, Fam A (2020) The effect of tube damage on flexural strength of±55 angle-ply concrete-filled FRP tubes. Constr Build Mater 240:117948
Mirmiran A, Shahawy M (1996) A new concrete-filled hollow FRP composite column. Compos Part B Eng 27:263–268
Qasrawi Y, Heffernan PJ, Fam A (2015) Dynamic behaviour of concrete filled FRP tubes subjected to impact loading. Eng Struct 100:212–225
Rafiee R (2016) On the mechanical performance of glass-fibre-reinforced thermosetting-resin pipes: A review. Compos Struct 143:151–164. https://doi.org/https://doi.org/10.1016/j.compstruct.2016.02.037
Shao Y, Mirmiran A (2005) Experimental investigation of cyclic behavior of concrete-filled fiber reinforced polymer tubes. J Compos Constr 9:263–273
Teng J, Huang YL, Lam L, Ye LP (2007) Theoretical model for fiber-reinforced polymer-confined concrete. J Compos Constr 11:201–210
Xie P, Lin G, Teng JG, Jiang T (2020) Modelling of concrete-filled filament-wound FRP confining tubes considering nonlinear biaxial tube behavior. Eng Struct 218:110762. https://doi.org/https://doi.org/10.1016/j.engstruct.2020.110762
Xing J, Geng P, Yang T (2015) Stress and deformation of multiple winding angle hybrid filament-wound thick cylinder under axial loading and internal and external pressure. Compos Struct 131:868–877. https://doi.org/https://doi.org/10.1016/j.compstruct.2015.05.036
Zohrevand P, Mirmiran A (2013) Seismic response of ultra-high performance concrete-filled FRP tube columns. J Earthq Eng 17:155–170